Supporting Information

Two Heads are Better than One: Improving Magnetic Relaxation in the Dysprosium Metallocene $DyCp^*_2BPh_4$ Upon Dimerization by Use of an Exceptionally Weakly-Coordinating Anion

Dylan Errulat,[a] Bulat Gabidullin,[b] Akseli Mansikkamaki[c] and Muralee Murugesu[a]*

[a] Department of Chemistry and Biomolecular Sciences, University of Ottawa, Ottawa, ON K1N 6N5, Canada.

[b] Canadian Light Source Inc. Saskatoon, SK S7N 2V3, Canada.

[c] NMR Research Unit, University of Oulu, P. O. Box 3000, 90014 Oulu, Finland.

*Corresponding Author: M. Murugesu (E-mail: m.murugesu@uottawa.ca)

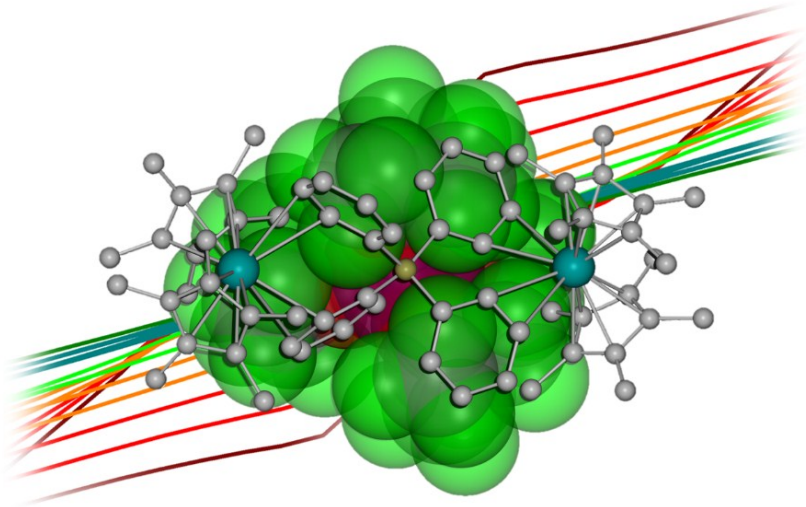

Table of Contents

Materials and Methods

All operations were performed in an Mbraun glovebox under an N_2 atmosphere or using standard Schlenk techniques unless otherwise stated. Solvents were dried using a J.C. Meyer solvent system and degassed by free-pump-thaw method, after which the solvents were stored over activated 4 Å molecular sieves prior to use. $DyCp^*_2(BPh_4)$ was prepared according to well-established literature procedure.[1] Anhydrous $DyCl_3$ was purchased from Strem Chemicals in 99.9% purity. $KN(SiMe_3)_2$ and $MgCl(C_3H_5)$ (2.0M in THF) were purchased from Sigma Aldrich and used as received. HCp* (99+%) was purchased from Alfa Aesar and was degassed/dried as above before use. $[Li][Al(OC(CF_3)_3)_4]$ was synthesized following previously published procedures.[2,3] $LiAlH_4$ was purchase from Alfa Aesar and $(CF_3)_3COH$ was obtained from Oakwood Chemical. It should be noted that in order to supplant the use of a glycol chiller in the original published procedure, a modification was employed involving the use of a Friedrich-style condenser cooled to 0°C with a circulating water pump as well as increasing the reactant equivalents of the alcohol (6-8 eq) which allowed for the reaction to proceed to completion. FT-IR spectra were recorded on a Nicolet Nexus 550 FT-IR spectrometer in the transmission window of 4000-400 cm^{-1} and the sample prepared under inert conditions between NaCl plates. Elemental Analysis was performed by Midwest Microlab.

Synthesis of $[Dy_2Cp^*_4(\mu\text{-}BPh_4)][Al(OC(CF_3)_3)_4]$ (1) A thick-walled bomb-type flask was charged with 301mg (0.4 mmol) of $DyCp^*_2BPh_4$ and 195mg (0.2 mmol) $[Li][Al(OC(CF_3)_3)_4]$ in 20 mL of toluene. The flask was evacuated briefly and brought to the vapor pressure of the solvent. The mixture was sonicated for 16 h, during which the temperature of the water bath reached as high as 60°C. The resulting yellow/orange solution was filtered through a fine fritted glass funnel and the solvent removed under reduced pressure to *ca.* 10 mL, after which a dense oil could be observed. From this oil, large yellow needles were obtained after standing at room temperature for up to several days (204 mg, 42%). To promote crystallization of the oil, it proved useful to seed subsequent reactions with crystals of **1** once obtained. CH Anal. Calcd. for $C_{101}H_{104}AlBDy_2F_{36}O_4$: C, 49.95; H, 4.32. Found: C, 47.14; H, 4.30. IR (cm^{-1}): 536 (w), 560 (w), 591 (w), 612 (m), 695 (m), 725 (s), 781 (w), 820 (s), 832 (m), 877 (w), 972 (s), 1019 (w), 1042 (w), 1062 (w), 1081 (w), 1160 (w), 1217 (m), 1239 (w), 1275 (m), 1300 (w), 1348 (m), 1429 (w), 1580 (w), 1604 (w), 2736 (w), 2865 (w), 2916 (w), 2972 (w), 3024 (w), 3057 (w).

Structural and X-ray Crystallography Details

Data collection was obtained on Bruker KAPPA APEX II diffractometer at the University of Ottawa equipped with a sealed Mo tube source (λ = 0.71073 Å) and APEX II CCD detector. A suitable crystal of $[Dy_2Cp^*_4(\mu\text{-}BPh_4)][Al(OC(CF_3)_3)_4]$ was mounted on a thin glass fiber, affixed using paraffin oil, and cooled to 200 K during data collection. Absorption correction was applied by semi-empirical method with the SADABS software. The structure was solved with SHELXT[4] and refined by full matrix least-squares methods on F^2 with SHELXL[5]. Direct methods were used to yield all nonhydrogen atoms which were refined with anisotropic thermal parameters, while hydrogen atom positions were calculated based on the geometry of their respective atoms. Supplementary crystallographic data for **1** can be obtained free of charge from the Cambridge Crystallographic Data Center at CCDC 1979114.

Table S1. Crystallographic data and selected data collection parameters.

Parameters	$[Dy_2Cp^*_4(\mu\text{-}BPh_4)][Al(OC(CF_3)_3)_4]$
Empirical formula	$C_{101}\ H_{104}\ Al_1\ B_1\ Dy_2\ F_{36}\ O_4$
Formula weight	2428.63
Crystal size, mm	0.638 x 0.216 x 0.197
Crystal system	Monoclinic
Space group	$P2_1/c$
Z	4
a, Å	15.5064(11)
b, Å	21.8874(16)
c, Å	31.229(2)
α, °	90
β, °	101.8170(10)
γ, °	90
Volume, $Å^3$	10374.4(13)
Calculated density, Mg/m^3	1.555
Absorption coefficient, mm^{-1}	1.552
T (K)	200(2)
F(000)	4864
Θ range for data collection, °	1.342 to 28.365
Limiting indices	h = ±20, k = ±29, l = ±41
Reflections collected / unique	152711 / 25882
R(int)	0.0386
Completeness to Θ = X, %	25.242, 100
Max. and min. transmission	0.7456 and 0.5574
Data / restraints / parameters	25882 / 1175 / 1650
Goodness-of-fit on F^2	1.110
Final R indices [I>2σ(I)][a]	R1 = 0.0395, wR2 = 0.0923
R indices (all data)	R1 = 0.0607, wR2 = 0.1080
Largest diff. peak/hole, e·$Å^3$	1.576 and -0.705

[a]$R = R_1 = \sum||F_0| - |F_c||/ \sum|F_0|$; $wR_2 = \{\sum[w\ (F_0^2 - F_c^2)^2/\sum[w(F_0)^2]]^{1/2}$; $w = 1/[\delta^2(F_o^2) + (ap)^2 + bp]$, where $p = [\max\ (F_0^2, 0) + 2F_c^2]/3$

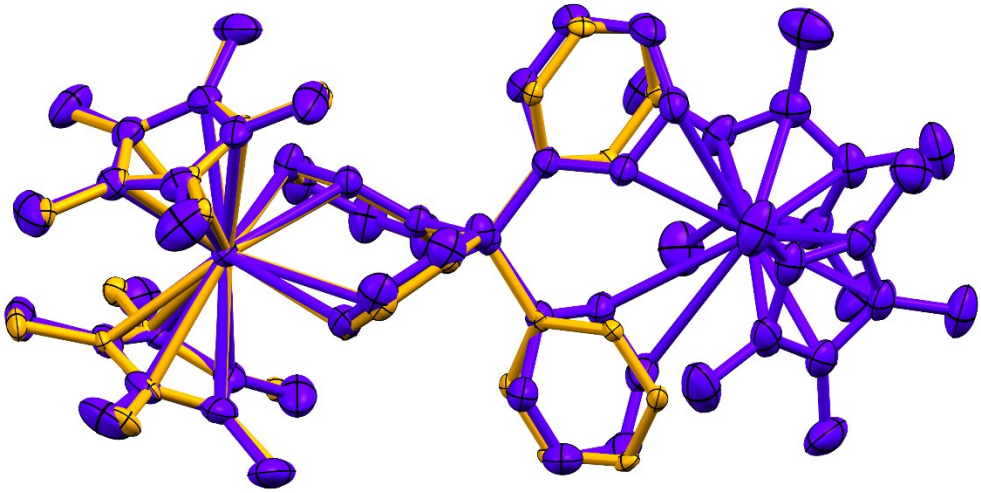

Figure S1. Structural overlay (RMS = 0.0271) of the monomeric Dy $Cp^*_2BPh_4$ (orange – Dy1 from CCDC 944005) and $[Dy_2Cp^*_4(\mu\text{-}BPh_4)]^+$ (**1** - blue) highlighting structural similarities between the two complexes. Hydrogen atoms have been omitted for clarity.

Magnetic Measurements. Magnetic susceptibility measurements were obtained using a Quantum Design SQUID magnetometer MPMS-XL7 operating between 1.8 and 300 K. DC measurements were performed on 14 mg of crushed polycrystalline sample, which was restrained with silicon grease and sealed in a polyethylene membrane under an inert atmosphere for which diamagnetic corrections were applied. The samples were subjected to DC fields of -7 to 7 T, and a 3.78 Oe driving field was used for AC measurements.

DC Magnetic Measurements for $[Dy_2Cp^*_4(\mu\text{-}BPh_4)][Al(OC(CF_3)_3)_4]$

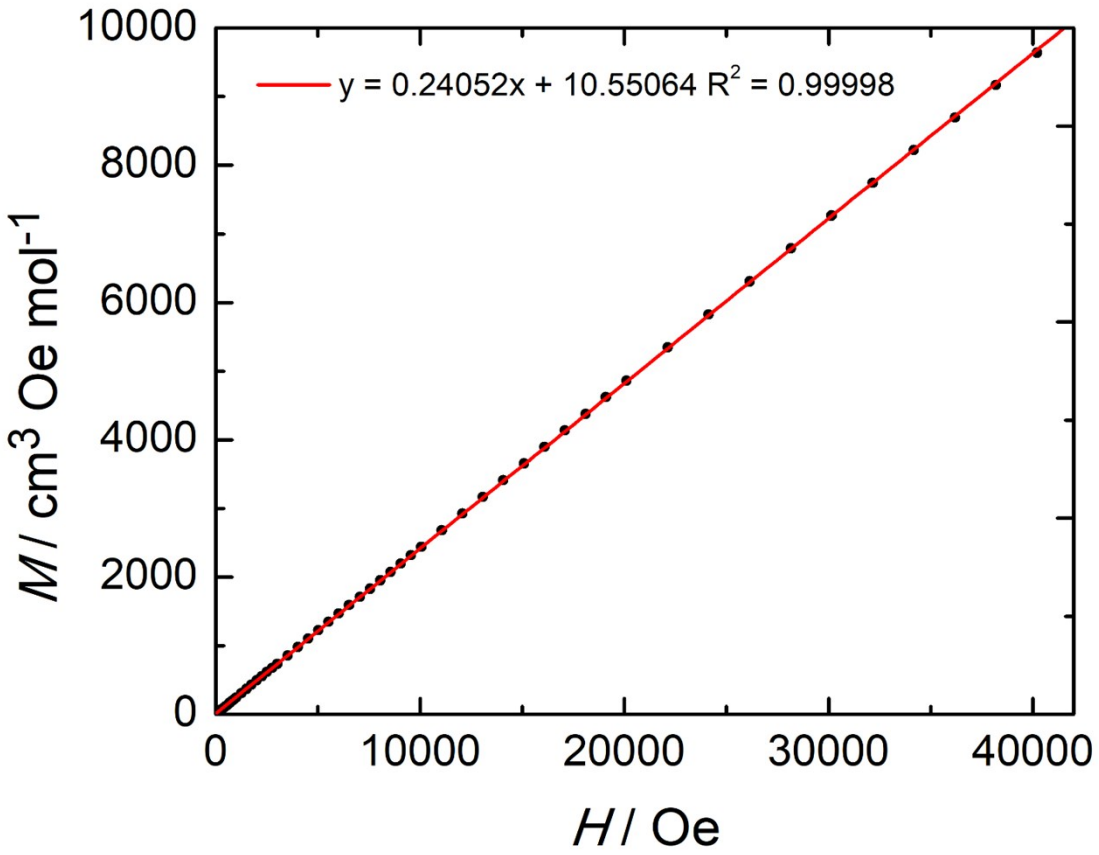

Figure S2. Magnetization data collected at 100 K to check for presence of ferromagnetic impurities. Linear fit of the data indicates the absence of impurities.

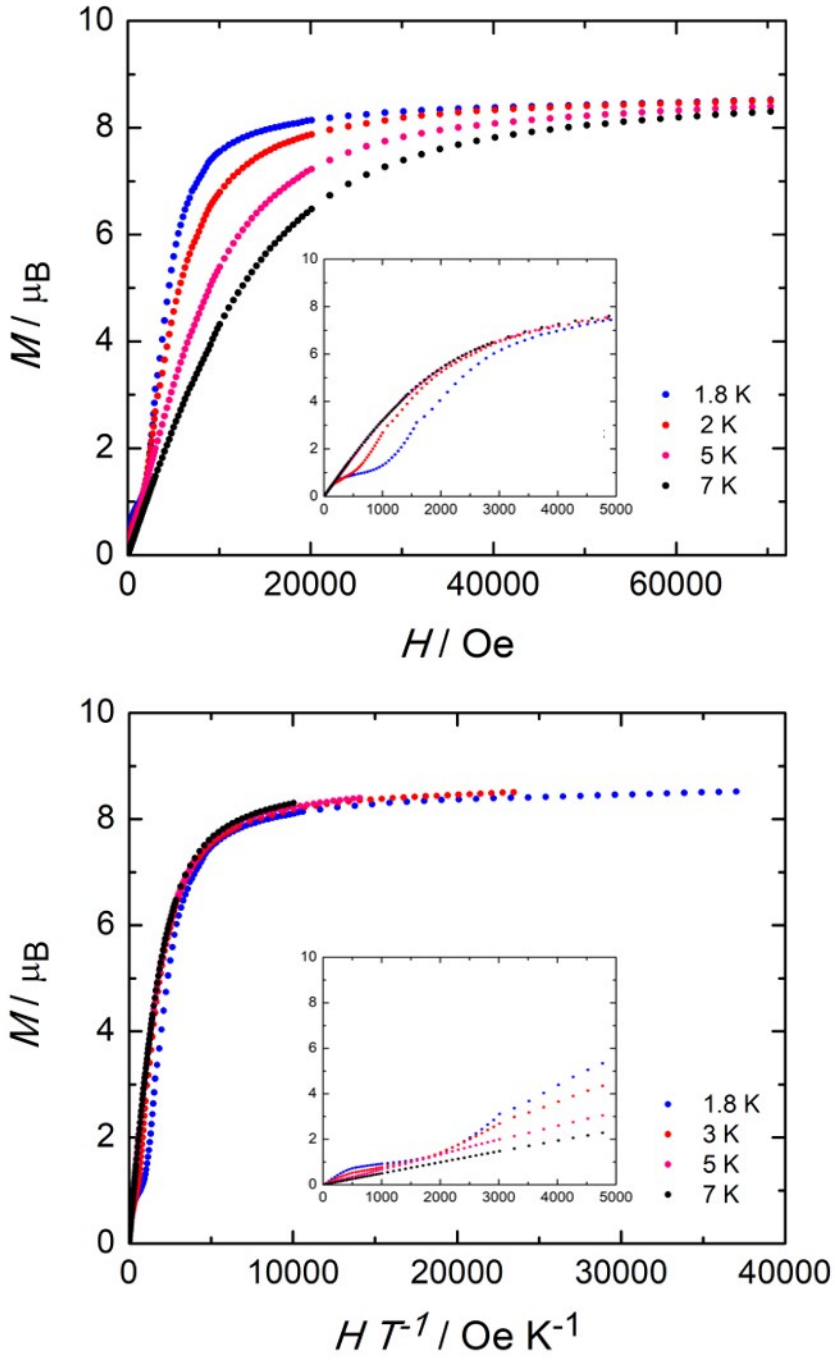

Figure S3. Field dependence of the magnetization (*top*) and the reduced magnetization (*bottom*) collected from 1.8 – 7 K. The insets highlight the behavior at low fields.

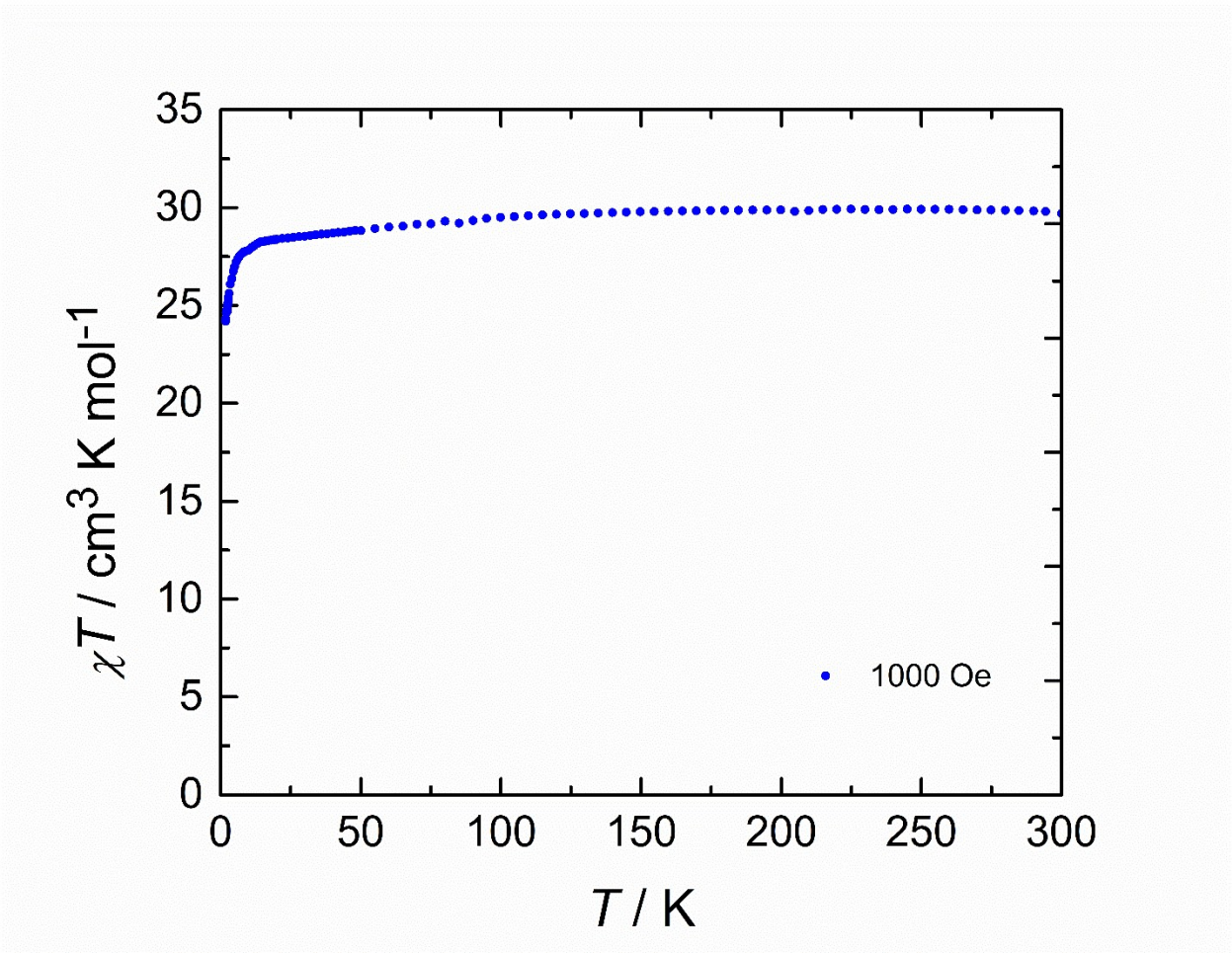

Figure S4. Temperature dependence of the χT product under an applied dc field of 1000 Oe, where χ is the molar magnetic susceptibility as defined by *M/H*

AC Magnetic Measurements for $[Dy_2Cp^*_4(\mu\text{-}BPh_4)]\ [Al(OC(CF_3)_3)_4]$

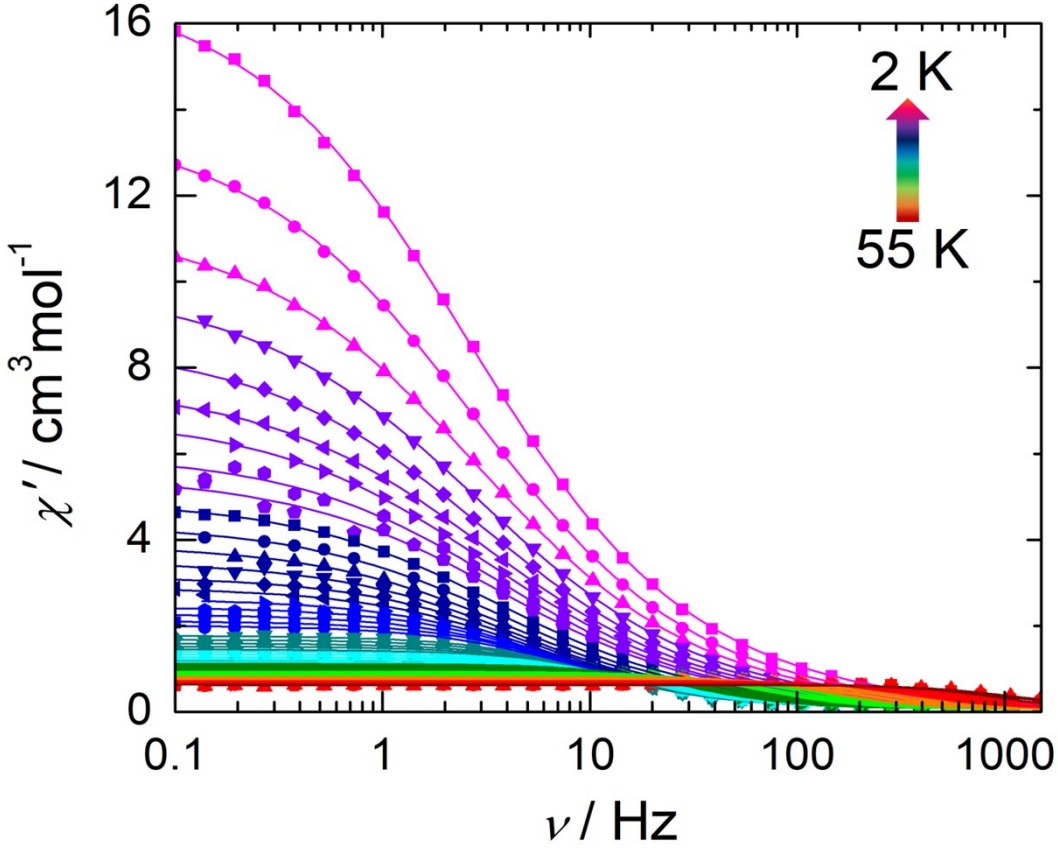

Figure S5. Frequency dependence of the in-phase magnetic susceptibility (χ') as a function of temperature in the range 2 – 55 K in the absence of an applied static field (H_{dc} = 0 Oe). Solid lines represent fits to the generalized Debye model. Parameters are summarized in Table S2.

Table S2. Best-fit parameters to the generalized Debye model for the frequency dependence of the in-phase magnetic susceptibility (χ') as a function of temperature (Figure S5). Data collected in the absence of an applied static field (H_{dc} = 0 Oe) in the range of 2 – 55 K.

T (K)	τ (s)	α	χ_S	χ_T
2	0.06066	0.38276	0	17.16259
2.5	0.05792	0.38233	0.00367	13.76818
3	0.05552	0.3792	0.02478	11.42603
3.5	0.05613	0.38725	0	9.96087
4	0.05302	0.37591	0.04328	8.60024
4.5	0.05129	0.37218	0.05019	7.64384
5	0.0502	0.36961	0.05388	6.90774
5.5	0.04413	0.35142	0.07729	6.02688
6	0.04277	0.35258	0.06911	5.5194
7	0.04406	0.34786	0.07451	4.95214
8	0.04193	0.33838	0.07844	4.38285
9	0.03878	0.32312	0.08093	3.9074
10	0.03546	0.30259	0.09376	3.50967
11	0.03164	0.28588	0.09377	3.16839
12	0.02924	0.27657	0.09808	2.90645
13	0.02593	0.25722	0.09577	2.64206
14	0.02375	0.22879	0.10282	2.44327
15	0.02181	0.22372	0.09562	2.28235
16	0.01979	0.19124	0.10881	2.11555
17	0.01834	0.20691	0.09109	2.01885
18	0.01987	0.19367	0.10783	2.12031
19	0.01551	0.14619	0.09995	1.77298
20	0.01438	0.13708	0.10598	1.68354
21	0.01309	0.13615	0.09863	1.59803
22	0.0115	0.13391	0.0805	1.52512
23	0.0111	0.11488	0.10003	1.45502
24	0.01007	0.1255	0.08876	1.4085
25	0.00917	0.10139	0.09633	1.3424
26	0.00834	0.0891	0.08743	1.27912
27	0.00743	0.07951	0.08982	1.22223
28	0.00694	0.11092	0.07839	1.21469
29	0.00628	0.06749	0.09127	1.15811
30	0.0055	0.06822	0.08751	1.12414
31	0.0049	0.04726	0.08122	1.08313
32	0.00433	0.057	0.08362	1.05415
33	0.00388	0.0288	0.0929	1.01597
34	0.00331	0.03147	0.09072	0.98547

35	0.00285	0.04484	0.0763	0.95962
36	0.00233	0.03722	0.06493	0.93472
37	0.00207	0.02393	0.07797	0.91078
38	0.00182	0.03734	0.0696	0.88799
39	0.0015	0.01615	0.0682	0.86228
40	0.00129	0.01504	0.07007	0.8436
41	0.00112	0.00298	0.07488	0.82393
42	9.2503E-4	0.03591	0.061	0.80549
43	8.2178E-4	0.00442	0.07376	0.78684
44	6.54757E-4	0.02685	0.04627	0.77071
45	6.22117E-4	0.00336	0.07937	0.75704
46	4.8216E-4	0.03211	0.03592	0.73978
47	4.69712E-4	0	0.09352	0.72434
48	3.64637E-4	0.00127	0.05622	0.70362
49	3.0822E-4	0.02515	0.03341	0.6952
50	2.59482E-4	0.01947	0.02072	0.6763
51	2.67757E-4	0	0.10941	0.6696
52	2.23675E-4	0	0.11078	0.65206
53	1.8168E-4	0	0.06824	0.63971
54	1.77791E-4	0.03347	0.12926	0.6353
55	1.4721E-4	0	0.11783	0.62104

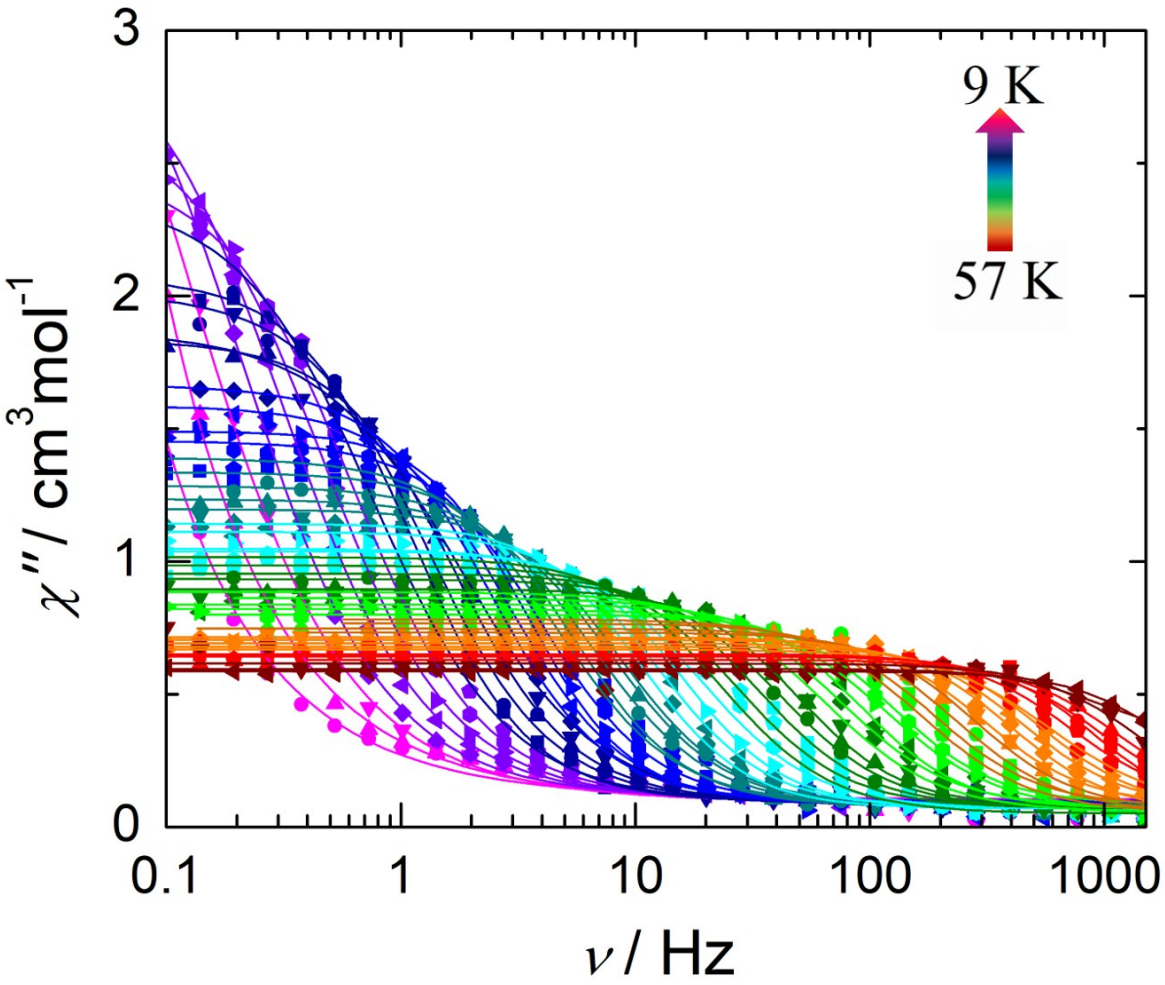

Figure S6. Frequency dependence of the in-phase magnetic susceptibility (χ') as a function of temperature in the range 9 - 57 K in the presence of an applied static field of 1000 Oe. Solid lines represent fits to the generalized Debye model. Parameters are summarized in Table S3.

Table S3. Best-fit parameters to the generalized Debye model for the frequency dependence of the in-phase magnetic susceptibility (χ') as a function of temperature (Figure S6). Data collected in the presence of an applied static field of 1000 Oe in the range of 9 – 57 K.

T (K)	τ (s)	α	χ_S	χ_T
9	5.39184	0.2098	0.09519	10.06276
10	1.26463	0.1753	0.09152	4.00636
11	0.75685	0.13898	0.10025	3.41277
12	0.50479	0.12965	0.09438	3.06883
13	0.34727	0.11078	0.09545	2.70263
14	0.2592	0.10021	0.09622	2.49827
15	0.21011	0.11959	0.08097	2.3927
16	0.14225	0.05321	0.0904	2.07649
17	0.12343	0.07872	0.08613	2.01892
18	0.09401	0.05809	0.09126	1.83945
19	0.08871	0.13274	0.06939	1.8773
20	0.06612	0.04619	0.09408	1.66651
21	0.05521	0.05264	0.08007	1.58878
22	0.04581	0.03163	1.49364	0.09082
23	0.04027	0.04343	0.0865	1.45564
24	0.03369	0.05864	0.08024	1.39166
25	0.02898	0.03442	0.07483	1.33706
26	0.02437	0.05746	0.07048	1.28662
27	0.02045	0.04792	0.07266	1.23541
28	0.01862	0.02797	0.08496	1.19724
29	0.01498	0.01319	0.06905	1.14192
30	0.01261	0.02554	0.0719	1.11272
31	0.00991	0	0.07435	1.03817
32	0.00849	0.04892	0.06539	1.04911
33	0.00692	0.04071	0.04939	1.01722
34	0.0059	0.03379	0.06983	0.98608
35	0.00475	0.02125	0.07455	0.95441
36	0.00389	0.03676	0.06678	0.9337
37	0.00321	0.00504	0.0782	0.8952
38	0.00248	0.05166	0.05299	0.88488
39	0.0021	0.03559	0.07253	0.86218
40	0.00174	0.00187	0.06858	0.83728
41	0.00138	0.05255	0.05617	0.82114
42	0.00124	0.00793	0.08592	0.7997
43	9.57663E-4	0.03615	0.05168	0.78246
44	8.54306E-4	0.01501	0.07898	0.76655
45	6.84219E-4	0.01682	0.05484	0.74675

46	5.41675E-4	0.04492	0.03995	0.73629
47	5.20163E-4	0	0.08519	0.71376
48	4.03325E-4	0.00802	0.05436	0.70545
49	3.52725E-4	0	0.07906	0.69065
50	2.91142E-4	0.00993	0.05968	0.67887
51	2.70931E-4	0.0384	0.07221	0.66885
52	2.2382E-4	0	0.09492	0.65104
53	1.86422E-4	0.00395	0.02738	0.64263
54	1.56089E-4	0.05361	0.06732	0.64187
55	1.36746E-4	0	0.07116	0.61536
56	1.2591E-4	0	0.12349	0.60751
57	1.38592E-4	0	0.28506	0.59471

Table S4. Best-fit parameters to the generalized Debye model for the frequency dependence of the out-of-phase magnetic susceptibility (χ'') as a function of temperature. Data collected in the absence of an applied static field (H_{dc} = 0 Oe) in the range of 2 – 55 K.

T (K)	τ (s)	α	χ_S	χ_T
2	0.05554	0.37047	0.09905	16.47565
2.5	0.05374	0.36865	0.08928	13.28507
3	0.05479	0.3694	0.14094	11.20372
3.5	0.05245	0.37019	0.03455	9.57152
4	0.05146	0.36698	0.01754	8.38297
4.5	0.04982	0.3608	0.03633	7.44337
5	0.04939	0.3625	0.01209	6.72965
5.5	0.04904	0.36299	0.13132	6.31305
6	0.04548	0.33379	0.00857	5.48503
7	0.0453	0.32673	0.81671	5.53811
8	0.04293	0.27982	0.02395	3.98681
9	0.03801	0.29226	0.00204	3.64764
10	0.03501	0.27301	0.73924	3.99966
11	0.0324	0.23087	0.00163	2.86821
12	0.03195	0.24976	2.71773	0.00328
13	0.02742	0.23841	0.02479	2.53538
14	0.02526	0.21861	0.00167	2.30567
15	0.02342	0.19744	0.01416	2.15483
16	0.02151	0.17792	0.03758	2.00907
17	0.01949	0.16611	0.01902	1.8728
18	0.01814	0.15885	0.00484	1.76463
19	0.0161	0.14739	0.01024	1.65974
20	0.0143	0.14265	0.00455	1.57876
21	0.01336	0.12494	0.00752	1.50186
22	0.01208	0.12019	0.07276	1.44926
23	0.01111	0.12653	7.27279E-4	1.38631
24	0.01023	0.11425	0.01342	1.33118
25	0.00983	0.09966	0.44347	1.67666
26	0.00873	0.08404	7.40989E-4	1.19328
27	0.00782	0.08024	0.00115	1.15918
28	0.00683	0.09116	2.23074E-4	1.1409
29	0.00631	0.08342	0.00398	1.08641
30	0.00552	0.07064	0.00133	1.04795
31	0.00481	0.06323	0.23444	1.23488
32	0.00434	0.05339	0.02245	0.99652
33	0.00371	0.06049	0.01515	0.97281
34	0.00329	0.03888	0.00229	0.91842

35	0.00275	0.06104	6.71299E-4	0.90495
36	0.00236	0.05422	0.00233	0.88232
37	0.00204	0.04578	0.00578	0.85856
38	0.0017	0.04683	6.36137E-4	0.83481
39	0.00157	0.01142	1.74875E-4	0.7914
40	0.00127	0.01695	6.44659E-4	0.78745
41	0.00107	0.02266	0.0286	0.78119
42	9.20403E-4	0.02766	4.71665E-4	0.75847
43	8.18618E-4	0.01496	0.00675	0.73346
44	6.70051E-4	0.02975	3.20311E-4	0.72139
45	5.8549E-4	0.06225	0.00339	0.72183
46	4.83566E-4	0.04414	0.00933	0.71152
47	4.23045E-4	0.04323	0.00649	0.69847
48	3.94911E-4	0	0	0.62424
49	3.00301E-4	0.05821	0.00324	0.67521
50	2.72173E-4	0.00391	0.00151	0.6407
51	2.47521E-4	0	0	0.60166
52	1.98413E-4	0.03428	0.00501	0.62954
53	1.71112E-4	0.01761	0.03047	0.63528
54	1.29776E-4	0.04956	0.01535	0.58768
55	1.35787E-4	0	4.97471E-11	0.53819

Table S5. Best-fit parameters to the generalized Debye model for the frequency dependence of the out-of-phase magnetic susceptibility (χ'') as a function of temperature. Data collected in the presence of an applied static field of 1000 Oe in the range of 9 – 57 K.

T (K)	τ (s)	α	χ_S	χ_T
9	1.73557	0.13614	0.72793	4.57784
10	1.00648	0.10918	0.0167	3.30663
11	0.66398	0.09136	0.02572	2.97611
12	0.45782	0.10783	0.01275	2.68947
13	0.32259	0.09143	0.09648	2.5198
14	0.24728	0.06771	0.0289	2.29351
15	0.19743	0.07907	0.0485	2.21344
16	0.14809	0.06548	0.08188	2.06803
17	0.11834	0.05329	1.53865E-5	1.84616
18	0.09782	0.06169	4.3355E-5	1.76404
19	0.08736	0.07485	0.00642	1.74047
20	0.06564	0.05209	0.00503	1.58309
21	0.05498	0.037	5.60272E-5	1.49047
22	0.04548	0	0.02588	1.38134
23	0.03989	0.04434	0.00558	1.3723
24	0.03445	0.03291	0.03295	1.32698
25	0.02908	0.02767	0.00118	1.24259
26	0.02516	0.01356	8.41402E-4	1.17286
27	0.02131	0.02	0.00101	1.13546
28	0.01743	0.03815	0.0114	1.14901
29	0.01526	0.0317	0.00723	1.08448
30	0.01271	0.02932	8.01434E-4	1.04383
31	0.0106	0.02185	0.00134	1.00157
32	0.0088	0.02005	0.00551	0.97043
33	0.00703	0.03865	7.97184E-4	0.9631
34	0.00575	0.03535	0.00949	0.94561
35	0.00491	0.0086	0.00169	0.86899
36	0.00398	0.00671	0.00384	0.84789
37	0.00318	0.02727	2.40586E-4	0.83934
38	0.00257	0.04096	0.00222	0.83474
39	0.00217	0.02418	0.00149	0.80775
40	0.00178	0.02017	2.13451E-4	0.77582
41	0.0014	0.04833	0.00313	0.77056
42	0.00118	0.02129	0.00233	0.75363
43	0.00101	0.03337	6.72632E-4	0.72284
44	8.05003E-4	0.01148	0.0405	0.72256
45	6.66868E-4	0.04597	3.41265E-4	0.70411

46	5.39456E-4	0	0.00588	0.67678
47	4.64051E-4	0.0126	0.02943	0.6829
48	3.81951E-4	0.04882	1.73252E-5	0.68078
49	3.37894E-4	0	0.0215	0.64351
50	3.07515E-4	0.01127	0.00922	0.63601
51	2.64564E-4	0.01262	0.01654	0.62709
52	2.11622E-4	0.02308	0.00276	0.61282
53	1.56081E-4	3.41354E-4	0	0.5988
54	1.42693E-4	0.04302	1.95385E-4	0.6277
55	1.43454E-4	0.00101	0.0222	0.55795
56	1.22343E-4	0.05287	0.02127	0.57382
57	7.83633E-5	0.08101	0.00119	0.65313

Table S6. Magnetic relaxation parameters obtained from the fit of the temperature dependent relaxation times for **1** compared to those obtained for $DyCp^*_2(BPh_4)$.[1] Best fits were obtained with contributions from Orbach, Raman and Quantum Tunneling relaxation pathways (Eqn. 1, *main text*).

		$[Dy_2Cp^*_4(\mu\text{-}BPh_4)][Al(OC(CF_3)_3)_4]$			
Parameters		**H_{dc} = 0 Oe**	**H_{dc} = 1000 Oe**	**H_{dc} = 0 Oe**	**H_{dc} = 1600 Oe**
QTM	τ_{QTM}	0.0493 s	-	0.0142 s	-
Orbach	τ_0	2.75×10^{-8} s	1.785×10^{-8} s	2×10^{-8} s	2×10^{-8} s
	U_{eff}	475 K / 330 cm^{-1}	490 K / 340 cm^{-1}	449 K / 312 cm^{-1}	452 K / 314 cm^{-1}
Raman	C	1.85×10^{-3} s^{-1} K^{-n}	1.50×10^{-4} s^{-1} K^{-n}	9×10^{-3} s^{-1} K^{-n}	5×10^{-4} s^{-1} K^{-n}
	n	3.38	3.86	3.17	3.85

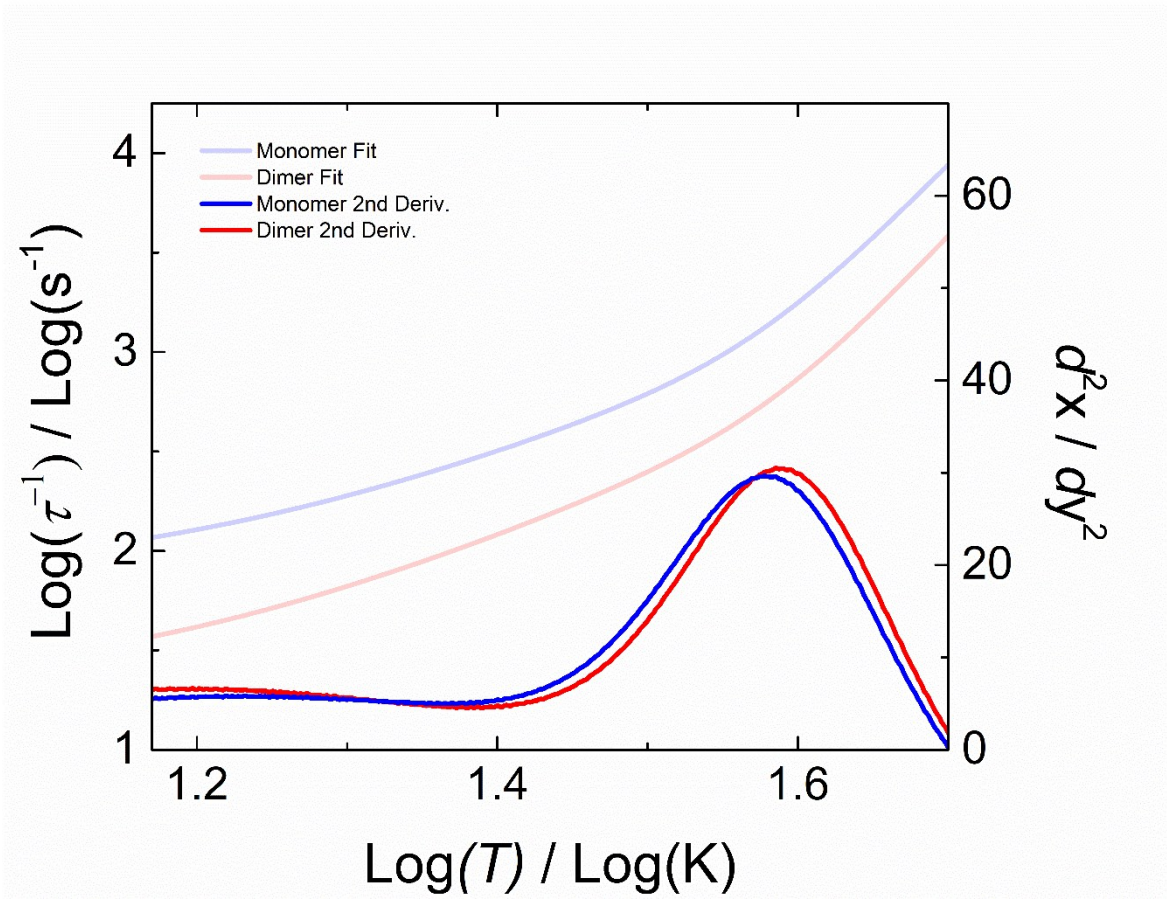

Figure S7. Relaxation rate data using the fitted parameters for **1** (red) compared to Dy $Cp^*_2(BPh_4)$ (blue) in the absence of an applied static field (*top*). The maxima of the second order derivative for the relaxation rate represents τ_{switch} (*bottom*).

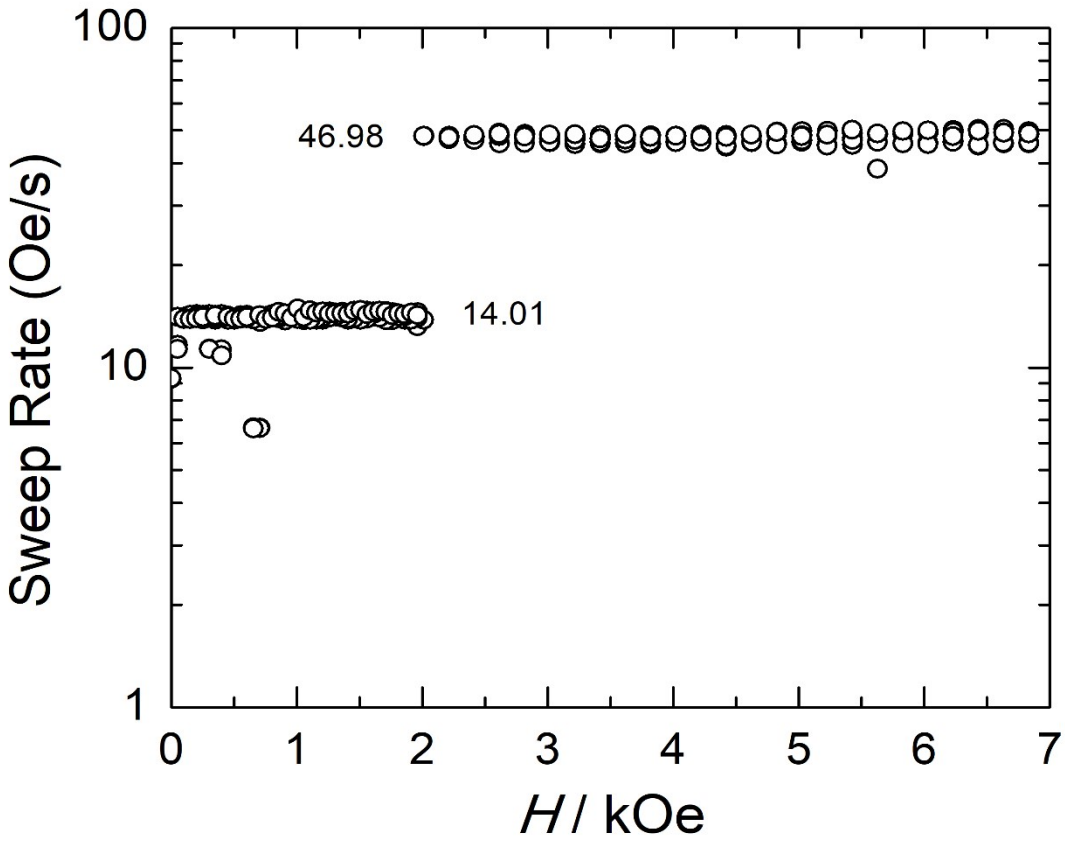

Figure S8. Sweep rate of the hysteresis measurement in seconds as a function of the applied field at an illustrative temperature of 2K. The average sweep rate in the region between 2 kOe and -2 kOe is 14.01 Oe s^{-1} while the rates at higher-fields is 46.98 Oe s^{-1}.

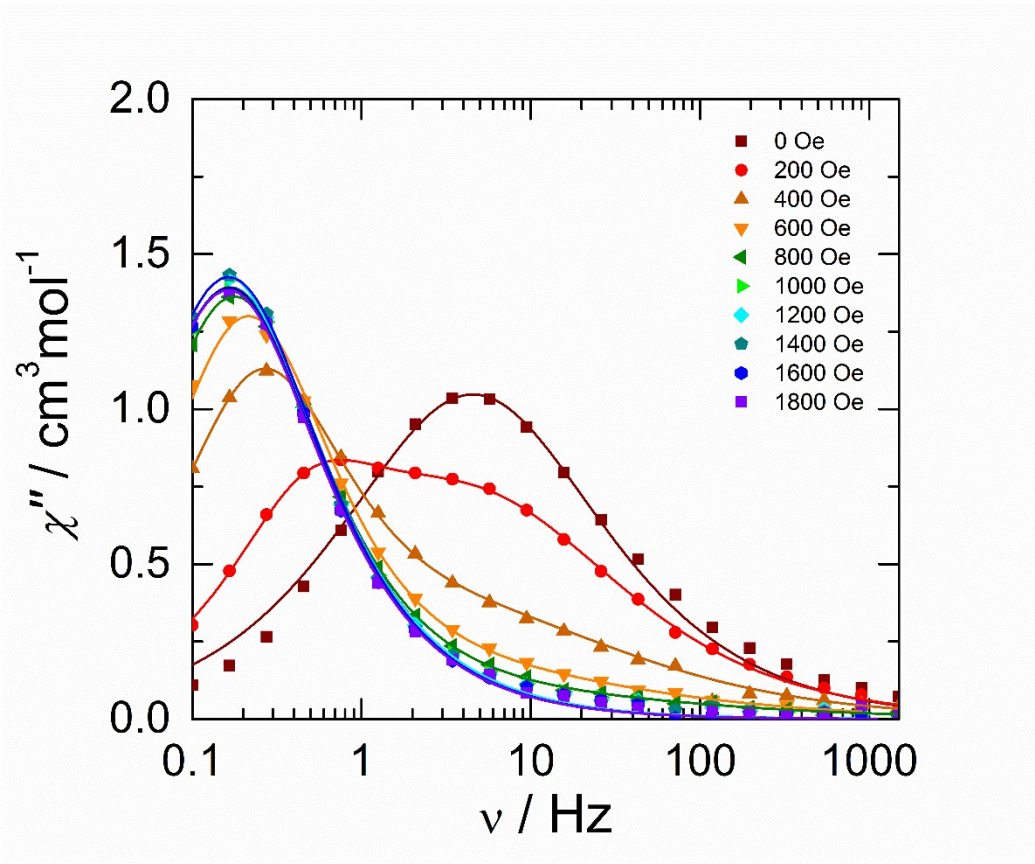

Figure S9. Frequency dependence of χ'' as a function of the applied field of 0 – 1800 Oe in increments of 200 Oe at a constant temperature of 10 K. Solid lines represent best fits to the generalized Debye model. Fit parameters are summarized in Table S7.

Table S7. Best-fit parameters to the generalized Debye model for the frequency dependence of the out-of-phase magnetic susceptibility (χ") as a function of field collected at a temperature of 10 K (Figure S9). Note that a Debye model invoking two separate processes was required to fit the fields from 200-800 Oe.

H (Oe)	τ_1 (s)	α_1	χ_{S1}	χ_{T1}	τ_2 (s)	α_2	χ_{S2}	χ_{T2}
0					0.03501	0.27301	0.73924	3.99966
200	0.33049	0	0.39485	1.34451	0.03048	0.33791	0	2.29743
400	0.62847	0.05136	0.7444	2.94189	0.02735	0.41652	0.41488	1.5134
600	0.7539	0.04223	0.00397	2.68781	0.02278	0.45472	0.579	1.0516
800	0.9059	0.06794	1.00512	3.99488	0.01465	0.49474	0.01177	0.29082
1000	0.95169	0.09485	1.60362	4.83993				
1200	1.03919	0.10648	1.21309	4.60829				
1400	0.96868	0.08299	1.00646	4.25752				
1600	0.96372	0.08001	1.10622	4.2652				
1800	0.97458	0.08342	1.68137	4.83946				

Ab Initio Calculations

The geometries used in the calculations were extracted directly from the crystal structure, consisting of two $[DyCp^*_2]^+$ cations and the bridging $[BPh_4]^-$ anion. The positions of the hydrogen atoms were optimized using density functional theory while the heavier atoms were kept frozen to their crystal structure coordinates. The DFT calculations were carried out using the Gaussian 09 quantum chemistry software revision E.01[6] and the hybrid PBE0 exchange-correlation (XC) functional.[7–9] A 4*f*-in-core MWB55 effective core potential (ECP) along with a corresponding valence basis set[10,11] was used for the Dy ions and Ahlrichs' valence-polarized triple-ζ basis[12] was used for other atoms. The quality of the integration grid was set to "UltraFine" in Gaussian and the accuracy of two-electron integrals was raised to 10^{-12} atomic units.

State-averaged complete active space self-consistent field (SA-CASSCF) calculations[13–17] were then carried out on both Dy^{III} ions in the asymmetric unit. In each calculation the other Dy^{III} ion was replaced by a diamagnetic Y^{III} ion. The active space consisted of the nine 4*f* electrons and the seven 4*f* orbitals. For both centers all 21 sextet, 224 quartet and 490 doublet roots were solved in three separate calculations. Spin-orbit coupling (SOC) was then introduced using the spin-orbit restricted active space state interaction (SO-RASSI) approach[18] where the SOC operator was constructed in a basis of CASSCF eigenstates using the atomic mean-field integral (AMFI) formalism[19,20] and then diagonalized to yield the spin-orbit coupled eigenstates and energies. All 21 sextets and the lowest 128 quartetes and 130 doublets (corresponding to an energy cut-off of 50,000 cm^{-1}) were included in the SO-RASSI calculation. The static magnetic properties (**g**-tensors), CF parameters and effective barrier for the relaxation of magnetization were calculated using the SINGLE_ANISO module.[21,22] Dipolar coupling was calculated using the POLY_ANISO routine within the point-dipolar approximation.[23,24] The dipolar coupling parameter was calculated by considering an Ising-type Hamiltonian acting on the projections of two S = ½ pseudospin doublets corresponding the ground KDs of ions 1 and 2:

$$\hat{H} = -J\,\tilde{S}_{z'1}\tilde{S}_{z'2}$$

The coupling parameter was then extract from the eigenvalues of the dipolar interaction. The coupling was extracted as twice the energy difference between the two lowest-energy doublets. It should be noted that the doublets are weakly split and the interaction does not therefore

correspond to an ideal Ising-type interaction. The splitting is however extremely weak and of the order 10^{-8} cm^{-1}.

The SA-CASSCF calculations were conducted with the Molcas quantum chemistry software version 8.2[25] and the SO-RASSI calculations using the OpenMolcas software version 18.11. Roos' relativistically contracted atomic natural orbital basis sets (ANO-RCC) were used throughout.[26–29] A polarized valence quadruple-ζ (VQZP) quality basis was used for the Dy ions, polarized valence triple-ζ (VTZP) quality bases were used for the carbon atoms in the Cp rings and the $[BPh_4]^-$ anion and the boron atom, polarized valence double-ζ (VDZP) quality bases were used for the remaining carbon atoms, the yttrium ion and the hydrogen atoms in the $[BPh_4]^-$ anion while a valence double- ζ (VDZ) basis was used for the remaining hydrogen atoms. Scalar relativistic effects were introduced using the scalar version of the exact two-component (X2C) transformation[30–32] as implemented in Molcas. Cholesky decomposition with a threshold of 10^{-8} atomic units was used in storage of the two-electron integrals.

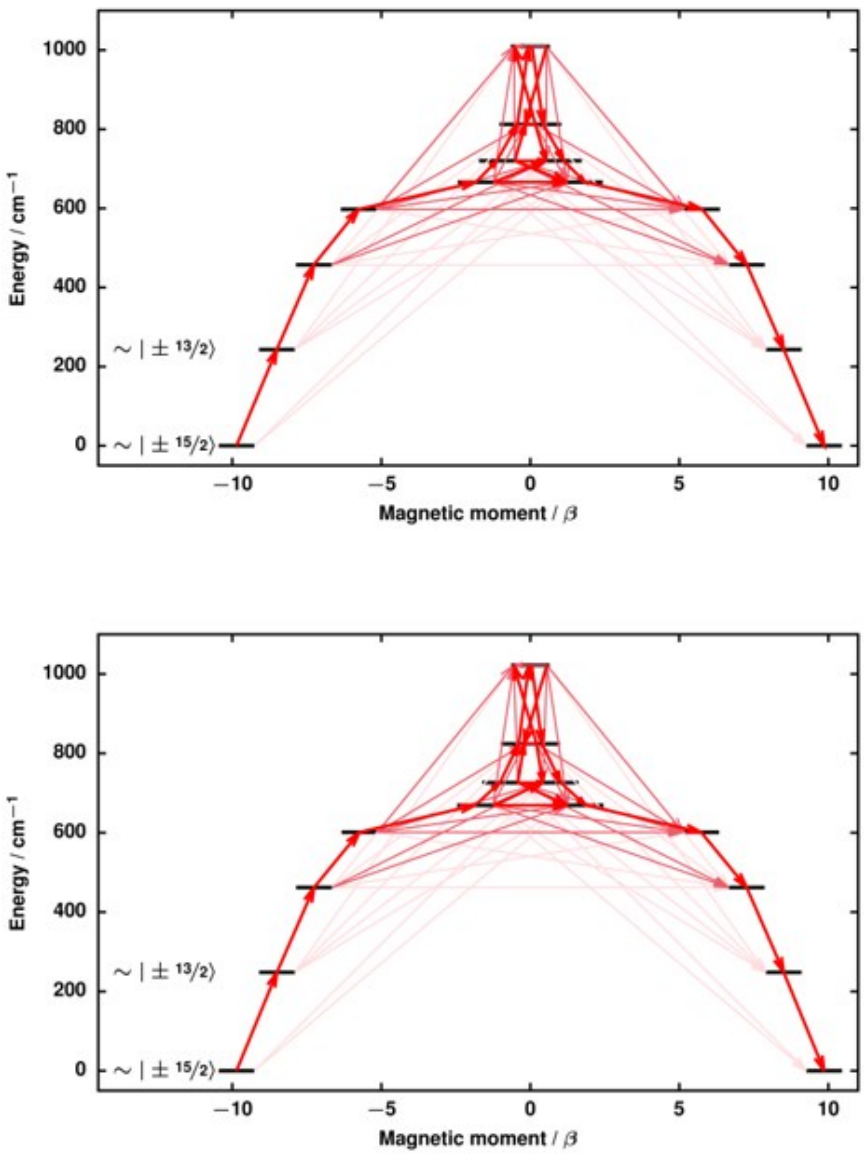

Figure S10. Qualitative barriers for the relaxation of magnetization in the Dy1 (*top*) and Dy2 (*bottom*) ions in **1**. Stronger lines indicate larger magnitudes of the transition magnetic moment between the respective states.

Table S8. Energies and principal components of the **g**-tensors of the eight lowest Kramers doublets (KDs) of the two Dy^{III} ions in **1**

	E / cm^{-1}	g_x	g_y	g_z	θ [a]
KD1	0	0.00054	0.00080	19.72091	0.0°

KD2	248	0.00765	0.00806	17.00843	0.9°
KD3	462	0.06549	0.07220	14.53032	2.1°
KD4	601	1.09564	1.37594	11.46738	0.9°
KD5	669	3.64445	5.69591	12.09804	87.7°
KD6	726	1.41352	1.98036	11.41005	92.7°
KD7	824	0.78512	1.49218	15.72756	89.9°
KD8	1022	0.01371	0.01903	19.49128	90.3°

	E / cm^{-1}	g_x	g_y	g_z	θ [a]
KD1	0	0.00059	0.00087	19.71574	0.0°
KD2	243	0.00827	0.00855	17.01509	1.3°
KD3	457	0.06270	0.06866	14.54743	2.6°
KD4	598	1.01483	1.22823	11.52824	0.9°
KD5	666	3.60513	5.53046	12.47648	91.2°
KD6	720	1.45980	2.15792	11.19976	86.7°
KD7	813	0.86882	1.69059	15.59821	90.1°
KD8	1009	0.00837	0.01454	19.50048	89.7°

[a] The angle between the principal magnetic axis of the given doublet and the that of the ground doublet.

Table S9. *Ab initio* crystal-field[33] parameters (in cm^{-1}) calculated for two Dy^{III} ions in **1** listed in the Iwahara–Chibotaru notation[34,35].

		First Dy^{III} ion			Second Dy^{III} ion		
k	q [a]	Re(B_{kq})	Im(B_{kq})	$\|B_{kq}\|$	Re(B_{kq})	Im(B_{kq})	$\|B_{kq}\|$

2	0	–532.744993	0.000000	532.744993	–527.710312	0.000000	527.710312
2	1	–6.066939	–0.989673	6.147130	–7.442991	2.326159	7.798021
2	2	117.319704	–13.076573	118.046219	114.334190	–3.331894	114.382729
4	0	–20.925134	0.000000	20.925134	–21.258926	0.000000	21.258926
4	1	–0.407161	–0.365865	0.547391	–0.200017	–0.094230	0.221102
4	2	–0.963080	0.022341	0.963339	–0.381023	0.515931	0.641376
4	3	–5.728847	–2.214108	6.141820	–6.156473	–0.363259	6.167181
4	4	4.290209	1.300828	4.483085	4.540500	0.077137	4.541155
6	0	–1.250747	0.000000	1.250747	0.128095	0.000000	0.128095
6	1	1.265974	0.796615	1.495756	1.496558	–1.233535	1.939406
6	2	28.409205	0.225018	28.410096	28.623840	0.043892	28.623873
6	3	–1.630708	0.614477	1.742639	–1.791154	–0.096678	1.793761
6	4	–1.003763	0.074630	1.006533	–1.781825	0.268890	1.801999
6	5	–5.140072	–1.508099	5.356743	–5.304842	–0.633591	5.342545
6	6	3.775981	1.004363	3.907272	3.754967	0.324496	3.768962
8	0	0.380664	0.000000	0.380664	0.346997	0.000000	0.346997
8	1	–0.021102	–0.008579	0.022779	–0.026732	0.038401	0.046789
8	2	–0.926270	–0.010285	0.926328	–0.925282	–0.004697	0.925294
8	3	0.024889	–0.025468	0.035610	0.029040	0.017727	0.034023
8	4	–0.080921	0.007498	0.081268	–0.064215	–0.002498	0.064263
8	5	0.071816	0.021834	0.075062	0.074002	0.008216	0.074456
8	6	–0.023521	–0.006562	0.024419	–0.025231	–0.001455	0.025273
8	7	–0.018644	–0.004757	0.019241	–0.018925	–0.001692	0.019001
8	8	0.004877	0.000699	0.004927	0.004796	0.000269	0.004803
10	0	–0.006782	0.000000	0.006782	–0.006629	0.000000	0.006629
10	1	–0.003118	–0.003886	0.004983	–0.003872	0.002498	0.004608
10	2	–0.026149	0.000127	0.026150	–0.027439	0.000521	0.027444
10	3	–0.001204	–0.001142	0.001660	–0.001326	–0.000194	0.001340
10	4	–0.004112	0.000065	0.004113	–0.003472	0.000112	0.003474
10	5	0.000684	–0.000207	0.000715	0.000459	0.000282	0.000538
10	6	–0.001065	–0.000405	0.001139	–0.001276	0.000270	0.001304
10	7	–0.003480	–0.000843	0.003581	–0.003499	–0.000681	0.003564
10	8	0.004358	0.001456	0.004595	0.004484	0.000517	0.004514

10	9	–0.000906	–0.000568	0.001069	–0.001141	–0.000167	0.001153
10	10	0.000108	0.000096	0.000145	0.000073	–0.000021	0.000076
12	0	0.008972	0.000000	0.008972	0.009059	0.000000	0.009059
12	1	–0.000871	0.000506	0.001008	–0.000987	–0.000661	0.001188
12	2	0.000142	–0.000012	0.000143	0.000366	0.000070	0.000372
12	3	–0.000219	–0.000051	0.000225	–0.000216	–0.000132	0.000253
12	4	0.002275	0.000035	0.002275	0.002300	0.000053	0.002301
12	5	–0.000147	0.000081	0.000168	–0.000174	–0.000048	0.000180
12	6	0.000085	0.000021	0.000087	0.000073	–0.000026	0.000077
12	7	0.000049	0.000002	0.000049	0.000049	0.000025	0.000055
12	8	–0.000114	–0.000042	0.000121	–0.000111	–0.000014	0.000112
12	9	0.000037	0.000009	0.000038	0.000055	0.000002	0.000055
12	10	0.000020	0.000029	0.000035	0.000023	0.000015	0.000027
12	11	–0.000070	–0.000044	0.000083	–0.000078	–0.000017	0.000079
12	12	0.000042	0.000023	0.000048	0.000044	0.000007	0.000045
14	0	–0.000019	0.000000	0.000019	–0.000018	0.000000	0.000018
14	1	0.000003	0.000000	0.000003	0.000003	0.000000	0.000003
14	2	0.000002	0.000000	0.000002	0.000002	–0.000001	0.000002
14	3	0.000002	0.000000	0.000002	0.000002	0.000002	0.000003
14	4	–0.000010	–0.000001	0.000010	–0.000011	0.000000	0.000011
14	5	–0.000001	–0.000001	0.000001	0.000000	0.000000	0.000000
14	6	0.000003	0.000000	0.000003	0.000003	0.000000	0.000003
14	7	0.000002	0.000001	0.000002	0.000002	0.000000	0.000002
14	8	0.000000	0.000000	0.000000	0.000000	0.000000	0.000000
14	9	0.000000	0.000000	0.000000	0.000000	0.000000	0.000000
14	10	0.000000	0.000000	0.000000	0.000000	0.000000	0.000000
14	11	0.000000	0.000000	0.000000	0.000000	0.000000	0.000000
14	12	0.000000	0.000000	0.000000	0.000000	0.000000	0.000000
14	13	0.000000	0.000000	0.000000	0.000000	0.000000	0.000000
14	14	0.000000	0.000000	0.000000	0.000000	0.000000	0.000000

[a] The CF parameters are only listed for positive values of q. The values with negative q are given by $B_{k-q} = (-1)^q B_{kq}^*$.

Table S10. Squared magnitudes of the projections of the CF eigenstates onto angular momentum eigenstates characterized by a total angular momentum J = 15/2 and an angular momentum projection M

M	KD1		KD2		KD3		KD4		KD5		KD6		KD7		KD8	
–15/2	0.038	0.930	0.000	0.000	0.004	0.027	0.000	0.000	0.000	0.000	0.000	0.000	0.000	0.000	0.000	0.000
–13/2	0.000	0.000	0.973	0.001	0.000	0.000	0.014	0.010	0.000	0.000	0.000	0.000	0.000	0.000	0.000	0.000
–11/2	0.001	0.030	0.001	0.000	0.116	0.836	0.002	0.000	0.006	0.002	0.004	0.000	0.000	0.001	0.000	0.000
–9/2	0.000	0.000	0.024	0.000	0.000	0.003	0.525	0.389	0.005	0.028	0.001	0.016	0.001	0.006	0.001	0.001
–7/2	0.000	0.000	0.000	0.000	0.002	0.011	0.000	0.005	0.289	0.124	0.418	0.045	0.071	0.017	0.002	0.015
–5/2	0.000	0.000	0.000	0.000	0.000	0.000	0.027	0.012	0.039	0.061	0.029	0.262	0.093	0.363	0.089	0.024
–3/2	0.000	0.000	0.000	0.000	0.000	0.000	0.001	0.005	0.163	0.092	0.011	0.002	0.313	0.079	0.068	0.266
–1/2	0.000	0.000	0.000	0.000	0.000	0.001	0.009	0.001	0.064	0.126	0.015	0.195	0.014	0.042	0.423	0.110
1/2	0.000	0.000	0.000	0.000	0.001	0.000	0.001	0.009	0.126	0.064	0.195	0.015	0.042	0.014	0.110	0.423
3/2	0.000	0.000	0.000	0.000	0.000	0.000	0.005	0.001	0.092	0.163	0.002	0.011	0.079	0.313	0.266	0.068
5/2	0.000	0.000	0.000	0.000	0.000	0.000	0.012	0.027	0.061	0.039	0.262	0.029	0.363	0.093	0.024	0.089
7/2	0.000	0.000	0.000	0.000	0.011	0.002	0.005	0.000	0.124	0.289	0.045	0.418	0.017	0.071	0.015	0.002
9/2	0.000	0.000	0.000	0.024	0.003	0.000	0.389	0.525	0.028	0.005	0.016	0.001	0.006	0.001	0.001	0.001
11/2	0.030	0.001	0.000	0.001	0.836	0.116	0.000	0.002	0.002	0.006	0.000	0.004	0.001	0.000	0.000	0.000
13/2	0.000	0.000	0.001	0.973	0.000	0.000	0.010	0.014	0.000	0.000	0.000	0.000	0.000	0.000	0.000	0.000
15/2	0.930	0.038	0.000	0.000	0.027	0.004	0.000	0.000	0.000	0.000	0.000	0.000	0.000	0.000	0.000	0.000

M	KD1		KD2		KD3		KD4		KD5		KD6		KD7		KD8	
–15/2	0.168	0.800	0.000	0.000	0.031	0.001	0.000	0.000	0.000	0.000	0.000	0.000	0.000	0.000	0.000	0.000
–13/2	0.000	0.000	0.832	0.143	0.001	0.000	0.000	0.023	0.000	0.000	0.000	0.000	0.000	0.000	0.000	0.000
–11/2	0.006	0.026	0.001	0.000	0.936	0.015	0.000	0.003	0.004	0.004	0.003	0.000	0.000	0.000	0.000	0.000
–9/2	0.000	0.000	0.020	0.003	0.004	0.000	0.004	0.916	0.006	0.024	0.000	0.014	0.000	0.005	0.000	0.002
–7/2	0.000	0.000	0.000	0.000	0.011	0.000	0.002	0.005	0.180	0.225	0.457	0.018	0.081	0.001	0.013	0.004
–5/2	0.000	0.000	0.000	0.000	0.000	0.000	0.000	0.032	0.081	0.026	0.005	0.276	0.008	0.456	0.014	0.101
–3/2	0.000	0.000	0.000	0.000	0.000	0.000	0.005	0.000	0.085	0.170	0.011	0.000	0.387	0.007	0.288	0.047
–1/2	0.000	0.000	0.000	0.000	0.000	0.000	0.002	0.006	0.130	0.064	0.002	0.213	0.000	0.053	0.073	0.456
1/2	0.000	0.000	0.000	0.000	0.000	0.000	0.006	0.002	0.064	0.130	0.213	0.002	0.053	0.000	0.456	0.073
3/2	0.000	0.000	0.000	0.000	0.000	0.000	0.000	0.005	0.170	0.085	0.000	0.011	0.007	0.387	0.047	0.288

5/2	0.000	0.000	0.000	0.000	0.000	0.000	0.032	0.000	0.026	0.081	0.276	0.005	0.456	0.008	0.101	0.014
7/2	0.000	0.000	0.000	0.000	0.000	0.011	0.005	0.002	0.225	0.180	0.018	0.457	0.001	0.081	0.004	0.013
9/2	0.000	0.000	0.003	0.020	0.000	0.004	0.916	0.004	0.024	0.006	0.014	0.000	0.005	0.000	0.002	0.000
11/2	0.026	0.006	0.000	0.001	0.015	0.936	0.003	0.000	0.004	0.004	0.000	0.003	0.000	0.000	0.000	0.000
13/2	0.000	0.000	0.143	0.832	0.000	0.001	0.023	0.000	0.000	0.000	0.000	0.000	0.000	0.000	0.000	0.000
15/2	0.800	0.168	0.000	0.000	0.001	0.031	0.000	0.000	0.000	0.000	0.000	0.000	0.000	0.000	0.000	0.000

Table S11. Numerical values of the transition magnetic moments between various states in the eight lowest KDs of the two Dy^{III} ions in **1**.

		First Dy^{III} ion		Second Dy^{III} ion	
Initial KD	Final KD	Transition on the same side of the barrier	Barrier-crossing transition	Transition on the same side of the barrier	Barrier-crossing transition
KD1	KD1	3.2868	0.0002	3.2860	0.0002
KD2	KD2	2.8965	0.0026	2.9234	0.0028
KD3	KD3	2.5169	0.0230	2.5512	0.0219
KD4	KD4	1.9521	0.4123	1.9542	0.3739
KD5	KD5	0.9660	2.9428	0.8612	2.9837
KD6	KD6	0.8241	2.0842	0.9095	2.0339
KD7	KD7	0.2044	3.0232	0.1932	2.8932
KD8	KD8	3.3107	0.6067	3.2811	0.3982
KD1	KD2	1.7731	0.0004	1.7731	0.0005
KD2	KD3	2.3402	0.0035	2.3413	0.0038
KD3	KD4	2.7483	0.0422	2.7546	0.0376
KD4	KD5	2.5282	0.5223	2.5002	0.5096
KD5	KD6	1.3294	1.9529	1.2950	1.9538
KD6	KD7	2.1707	1.0014	2.2196	0.9853
KD7	KD8	1.2964	1.2496	1.2681	1.2398
KD1	KD3	0.2053	0.0003	0.2202	0.0002
KD2	KD4	0.2061	0.0058	0.2202	0.0054
KD3	KD5	0.1610	0.3246	0.1613	0.2929
KD4	KD6	1.7187	0.2923	1.7808	0.2775
KD5	KD7	0.4199	0.2605	0.4229	0.2764

KD6	KD8	0.2938	0.2875	0.2452	0.2716
KD1	KD4	0.2652	0.0020	0.2788	0.0019
KD2	KD5	0.1353	0.0262	0.1362	0.0208
KD3	KD6	0.0632	0.1545	0.0553	0.1361
KD4	KD7	0.0752	0.5833	0.0694	0.6027
KD5	KD8	0.1430	0.1705	0.1559	0.1682
KD1	KD5	0.0239	0.0518	0.0240	0.0500
KD2	KD6	0.1855	0.0293	0.1923	0.0302
KD3	KD7	0.0731	0.0573	0.0697	0.0579
KD4	KD8	0.1577	0.1471	0.1608	0.1624
KD1	KD6	0.0223	0.0396	0.0214	0.0360
KD2	KD7	0.0305	0.0958	0.0281	0.0936
KD3	KD8	0.0536	0.0267	0.0498	0.0332
KD1	KD7	0.0244	0.0090	0.0215	0.0083
KD2	KD8	0.0358	0.0127	0.0345	0.0131
KD1	KD8	0.0083	0.0030	0.0086	0.0021

References

1 S. Demir, J. M. Zadrozny and J. R. Long, *Chem. - Eur. J.*, 2014, **20**, 9524–9529.
2 I. Krossing and I. Raabe, *Angew. Chem. Int. Ed.*, 2004, **43**, 2066–2090.
3 I. Krossing, *Chem. – Eur. J.*, 2001, **7**, 490–502.
4 G. M. Sheldrick, *Acta Crystallogr. Sect. Found. Adv.*, 2015, **71**, 3–8.
5 G. M. Sheldrick, *Acta Crystallogr. Sect. C Struct. Chem.*, 2015, **71**, 3–8.
7 J. P. Perdew, K. Burke and M. Ernzerhof, *Phys Rev Lett*, 1997, **78**, 1396–1396.
8 J. P. Perdew, K. Burke and M. Ernzerhof, *Phys Rev Lett*, 1996, **77**, 3865–3868.
9 C. Adamo and V. Barone, *J Chem Phys*, 1999, **110**, 6158–6170.
10 M. Dolg, H. Stoll, A. Savin and H. Preuss, *Theor Chim Acta*, 1989, **75**, 173–194.
11 D. Andrae, U. Häußermann, M. Dolg, H. Stoll and H. Preuß, *Theor Chim Acta*, 1990, **77**, 123–141.
12 A. Schäfer, C. Huber and R. Ahlrichs, *J Chem Phys*, 1994, **100**, 5829–5835.
13 B. O. Roos, in *Advances in Chemical Physics: Ab Initio Methods in Quantum Chemistry II, Vol. 69*, ed. K. P. Lawley, Wiley, New York, NY, USA, 1987, pp. 399–455.
14 P. Siegbahn, A. Heiberg, B. Roos and B. Levy, *Phys Scr.*, 1980, **21**, 323–327.
15 B. O. Roos, P. R. Taylor and P. E. M. Siegbahn, *Chem Phys*, 1980, **48**, 157–173.
16 P. E. M. Siegbahn, J. Almlöf, A. Heiberg and B. O. Roos, *J Chem Phys*, 1981, **74**, 2384–2396.
17 B. O. Roos, R. Lindh, P. Åke Malmqvist, V. Veryazov and P.-O. Widmark, *Multiconfigurational Quantum Chemistry*, Wiley, Hoboken, NJ, USA, 2016.
18 P. AAke Malmqvist, B. O. Roos and B. Schimmelpfennig, *Chem Phys Lett*, 2002, **357**, 230–240.
19 B. A. Heß, C. M. Marian, U. Wahlgren and O. Gropen, *Chem Phys Lett*, 1996, **251**, 365–371.
20 O. Christiansen, J. Gauss and B. Schimmelpfennig, *Phys Chem Chem Phys*, 2000, **2**, 965–971.
21 L. F. Chibotaru and L. Ungur, *J Chem Phys*, 2012, 137, 064112.
22 L. Ungur and L. F. Chibotaru, in *Lanthanides and Actinides in Molecular Magnetism*, eds. R. A. Layfield and M. Murugesu, Wiley-VHC, Weinheim, Germany, 2015, pp. 153–184.
23 L. F. Chibotaru, L. Ungur and A. Soncini, *Angew Chem*, 2008, **120**, 4194–4197.
24 L. Ungur, W. van den Heuvel and L. F. Chibotaru, *New J Chem*, 2009, **33**, 1224–1230.
25 F. Aquilante, J. Autschbach, R. K. Carlson, L. F. Chibotaru, M. G. Delcey, L. De Vico, I. Fdez. Galván, N. Ferré, L. M. Frutos, L. Gagliardi, M. Garavelli, A. Giussani, C. E. Hoyer, G. Li Manni, H. Lischka, D. Ma, P. Åke Malmqvist, T. Müller, A. Nenov, M. Olivucci, T. B. Pedersen, D. Peng, F. Plasser, B. Pritchard, M. Reiher, I. Rivalta, I. Schapiro, J. Segarra-Martí, M. Stenrup, D. G. Truhlar, L. Ungur, A. Valentini, S. Vancoillie, V. Veryazov, V. P. Vysotskiy, O. Weingart, F. Zapata and R. Lindh, *J Comp Chem*, 2015, **37**, 506–541.
26 P.-O. Widmark, P.-Åke Malmqvist and B. O. Roos, *Theor Chim Acta*, 1990, **77**, 291–306.
27 B. O. Roos, R. Lindh, P.-Åke Malmqvist, V. Veryazov and and P.-O. Widmark, *J Phys Chem A*, 2004, **108**, 2851–2858.
28 Björn O. Roos, Roland Lindh, Per-Åke Malmqvist, Valera Veryazov and and P.-O. Widmark, *J Phys Chem A*, 2005, **109**, 6575–6579.

29 B. O. Roos, R. Lindh, P. AAke Malmqvist, V. Veryazov, P.-O. Widmark and A. C. Borin, *J Phys Chem A*, 2008, **112**, 11431–11435.
30 W. Kutzelnigg and W. Liu, *J Chem Phys*, , DOI:10.1063/1.2137315.
31 M. Filatov, *J. Chem. Phys.*, 2006, **125**, 107101.
32 D. Peng and M. Reiher, *Theor. Chem. Acc.*, 2012, **131**, 1081.
33 L. Ungur and L. F. Chibotaru, *Chem. – Eur. J.*, 2017, **23**, 3708–3718.
34 N. Iwahara and L. F. Chibotaru, *Phys Rev B*, 2015, **91**, 174438.
35 N. Iwahara, L. Ungur and L. F. Chibotaru, *Phys Rev B*, 2018, **98**, 054436.